# Total scatter factors of small beams: A multidetector and Monte Carlo study

Paolo Francescon,[a] Stefania Cora, and Carlo Cavedon
*Department of Medical Physics, ULSS 6, Vicenza, Italy*

(Received 20 June 2007; revised 12 November 2007; accepted for publication 3 December 2007; published 15 January 2008)

The scope of this study was to estimate total scatter factors ($s_{c,p}$) of the three smallest collimators of the Cyberknife radiosurgery system (5–10 mm in diameter), combining experimental measurements and Monte Carlo simulation. Two microchambers, a diode, and a diamond detector were used to collect experimental data. The treatment head and the detectors were simulated by means of a Monte Carlo code in order to calculate correction factors for the detectors and to estimate total scatter factors by means of a consistency check between measurement and simulation. Results for the three collimators were: $s_{c,p}(5\ \text{mm})=0.677\pm0.004$, $s_{c,p}(7.5\ \text{mm})=0.820\pm0.008$, $s_{c,p}(10\ \text{mm})=0.871\pm0.008$, all relative to the 60 mm collimator at 80 cm source-to-detector distance. The method also allows the full width at half maximum of the electron beam to be estimated; estimations made with different collimators and different detectors were in excellent agreement and gave a value of 2.1 mm. Correction factors to be applied to the detectors for the measurement of $s_{c,p}$ were consistent with a prevalence of volume effect for the microchambers and the diamond and a prevalence of scattering from high-$Z$ material for the diode detector. The proposed method is more sensitive to small variations of the electron beam diameter with respect to the conventional method used to commission Monte Carlo codes, i.e., by comparison with measured percentage depth doses (PDD) and beam profiles. This is especially important for small fields (less than 10 mm diameter), for which measurements of PDD and profiles are strongly affected by the type of detector used. Moreover, this method should allow $s_{c,p}$ of Cyberknife systems different from the unit under investigation to be estimated without the need for further Monte Carlo calculation, provided that one of the microchambers or the diode detector of the type used in this study are employed. The results for the diamond are applicable only to the specific detector that was investigated due to excessive variability in manufacturing.  [DOI: 10.1118/1.2828195]

Key words: small beams, total scatter factor, Monte Carlo, radiosurgery, Cyberknife

## I. INTRODUCTION

In recent years, the introduction of new technology in radiation therapy has improved the capability of treating small and irregular lesions. The possibility to provide better conformal dose distributions and more accurate and precise dose delivery offered by techniques such as IMRT, micromultileaf collimators, and image-guided systems such as the Cyberknife (Accuray, Inc., Sunnyvale, CA) and Tomotherapy (Tomotherapy, Inc., Madison, WI) has contributed to their diffusion to several centers. On the other hand, it has also raised the impact of dosimetry of small beams on treatment quality. In particular, the determination of total scatter factors ($s_{c,p}$) has a large influence on the calculation of monitor units of small beams. In fact, accuracy within ±3% is difficult to achieve for total scatter factors of small beams[1] and this strongly affects overall dosimetric accuracy, especially if reference levels on the order of ±5% shall be observed.[2]

Discrepancies in total scatter factor values have been reported for the smallest collimators of the Cyberknife radiosurgery system.[3–9] Such discrepancies might be explained as a contribution of several factors: differences in the choice of the dosimeters among centers, possible inaccuracies in the experimental setup (in particular for the 5 mm cone), and differences in beam parameters between units (in particular the electron beam width). In fact, it has been observed for other linear accelerators[10] that units with a similar design can have spot sizes that can differ up to 1 mm. This difference can have an impact on the measurement of total scatter factors for small cones, as it will be shown in the next section.

The problem of dosimetry of small beams has been investigated by several authors.[11–28] It is known that the main problems with the detectors are retraceable to their finite size compared to the small size of the beams and to the nonwater equivalence of the materials. Moreover, the dosimetry of small beams is complicated by the lack of lateral electronic equilibrium. For these reasons, many authors have proposed Monte Carlo (MC) systems as suitable tools for small beam commissioning.[1,29–35] The Monte Carlo method represents an "ideal" dosimeter because it can simulate energy deposition per each radiation particle in a given material. The BEAM code[36] has been used extensively and it has shown good agreement with experimental measurements for photon and electron beams.[37] A complete and updated review of papers dealing with output factors of small beams can be found in the recent work by Sauer *et al.*,[38] in which both experimental

TABLE I. Characteristics of the detectors used for measurement of total scatter factors.

| Detector | Type and dimension | Material | Characteristics |
|---|---|---|---|
| Exradin A16 | Thimble chamber collecting volume 0.007 $cm^3$, diameter 2.4 mm, | Walls and central electrode: C552 | Volume effect moderate polarity effect |
| PTW PinPoint 31014 | Thimble chamber collecting volume 0.015 $cm^3$, diameter 2.1 mm | PMMA, aluminum electrode | Volume effect moderate polarity effect |
| PTW diamond | 12 $mm^2$ front area 0.25 mm thickness | Carbon | Volume effect, variability in manufacturing |
| PTW 60012 *p*-type diode | 1 $mm^2$ front area 2.5 $\mu$m thickness | Silicon, polyethylene | Nontissue equivalence |

and Monte Carlo methods are taken into account.

The main goal of this work was to use the Monte Carlo method to calculate $s_{c,p}$ for the three smallest collimators of the Cyberknife radiosurgery system[39] and to obtain correction factors to be applied to raw $s_{c,p}$ data by using Monte Carlo simulations of the detectors used for measurement. Similar correction factors were defined in previous works for radiosurgery[11] and for IMRT.[31,40] However, since accuracy of Monte Carlo simulation depends on the choice of beam parameters such as energy, divergence, and radial distribution of the electron beam incident on the target,[41,42] a prerequisite of this study has been to obtain a means to infer source parameters and to choose the appropriate correction factor for a given detector and for a specific Cyberknife system, even if its beam characteristics do not strictly match those of the unit used for this study. The method to determine beam parameters for Monte Carlo simulation differed from the usual approach consisting of a comparison between measured and calculated depth dose curves and beam profiles, but took into account the actual shape and chemical composition of the detectors, as will be described in the next section. In this sense, in the proposed method experiment and simulation are intertwined and not subordinated to each other as a means to estimate scatter factors of small beams.

## II. MATERIAL AND METHODS

### II.A. Experimental measurements

Two microchambers and two solid state detectors were used to measure total scatter factors for the three smallest circular collimators available with the Cyberknife radiosurgery system (5, 7.5, and 10 mm at 80 cm from the source). The microchambers were the PTW PinPoint 31014 and the Exradin A16. The solid state detectors were the PTW 60012 unshielded diode and the PTW TM60003 diamond. The characteristics of diode and diamond detectors have been extensively studied and reported.[43–58] The characteristics of the detectors employed in this study are summarized in Table I. For the microchambers, the effective point of measurement was determined by comparison with the Exradin T14P parallel-plate chamber, whose effective point of measurement was assumed to lie on the inner surface of the upper plate. The effective point of measurement was determined to be at 2.2 and 3.7 mm from the external tip for the A16 and PinPoint chambers, respectively (the detectors were used with their stem parallel to the beam axis). The measurement was performed by comparing the point of maximum dose along the depth dose curve of the 5 mm collimator.

$s_{c,p}$ was defined as $D_{coll}/D_{60}$, where $D_{coll}$ was the dose measured with each collimator and $D_{60}$ was the reference dose measured with the 60 mm collimator. The effective point of measurement was placed at 80 cm from the source at 1.5 cm depth from the surface, corresponding to the point of maximum dose along the depth dose curve of the 60 mm collimator.

The diamond and diode detectors were also used with their stem parallel to the beam axis. The detectors were centered on the horizontal plane by means of a laser pointer, then their position was finely tuned (within ±0.2 mm) to achieve the maximum signal intensity using the 5 mm collimator. All measurements were made with 50 monitor units and averaged over a series of at least five repeated runs. The standard deviation between repeated measurements was less than 0.3% for the microchambers and less than 0.1% for the solid state detectors.

Since a polarity effect was observed with microchambers (±2.2% with respect to the average for the 5 mm collimator with the PinPoint chamber, ±1% with the A16), measurements were averaged between positive and negative polarities (+/− 400 V). These effects in general cannot be simulated by means of Monte Carlo because they are due to electrical phenomena that are not directly connected to dose absorption within the active volume of the detector.

As will be described in the Sec. II C, measurements of tissue-phantom ratios (TPR) and beam profiles were needed in order to fine-tune beam parameters in the Monte Carlo simulation, even if the method proposed will eventually be independent from profile matching (profiles were anyhow measured for verification purposes). TPRs were measured by means of the PTW 60012 diode. Profiles were measured with Gafchromic (ISP International Specialty Products, Wayne, NJ) film (EBT type) for the 5 mm collimator and with the PTW 31014 PinPoint microchamber for the 60 mm collimator. The films were read by means of a flat bed scanner (Epson 1680 Pro) used in the red channel after 24–48 h from exposition.

### II.B. Monte Carlo simulations

Monte Carlo simulation of the treatment head of the Cyberknife has been performed with the BEAMnrc code,[36] by using details of the geometry and material composition provided by the manufacturer. The geometry of the simulated

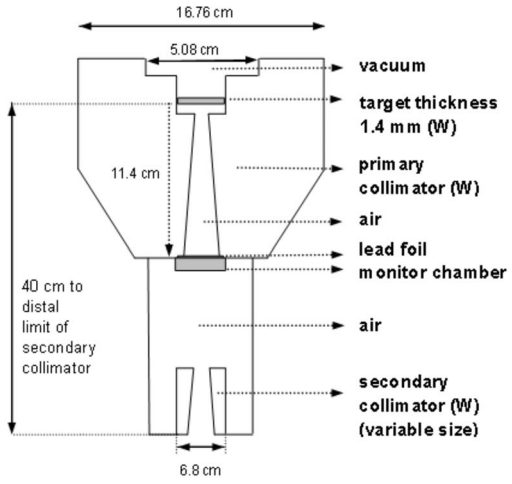


FIG. 1. Schematic of a Cyberknife treatment head. Components are not to scale, but relevant dimensions and materials are reported.

treatment head has been drawn in Fig. 1. The phase space obtained at the exit plane of each collimator has been used as an input source for the simulation of the detectors.

All BEAMnrc simulations used a transport and particle production threshold energy of 521 keV total energy for electrons (ECUT=AE=521 keV) and 10 keV for photons (PCUT=AP=10 keV). Electron range rejection with a "save energy" ESAVE=2 MeV was used. For improved simulation efficiency, the directional bremsstrahlung technique[59] was employed.

The average absorbed dose in the active volume of the detectors embedded in a water phantom has been calculated in order to obtain $s_{c,p}$ values to be compared with measured ones. The calculations were performed using the EGSnrc code[60,61] and the C++ class library, egspp, for use with the EGSnrc package, developed by Kawrakow.[62] The egspp class library also provides a general purpose geometry package that can be used to model a wide range of geometrical structures allowing a more accurate description of a detector. All simulations were performed until the achieved uncertainty was less than 0.15% (one standard deviation). The transport parameters used in the simulations were ECUT =512 keV (total energy for electrons), PCUT=1 keV (total energy for photons), ESTEPE=0.25, and XIMAX=0.5. The electron multiple scattering and boundary crossing algorithm was PRESTA-II. To improve simulation efficiency, a modification of the "range rejection" variance reduction technique[63] has been used: electrons that cannot enter the cavity region are subjected to a "Russian Roulette game" with a survival probability of $p$ instead of being range rejected. The weight of the survived electron is modified by a factor of $1/p$. Also the photons produced by these electrons are transported using a splitting factor of $1/p$.

The composition of the detectors has been simulated using PEGS4,[60] with a cutoff energy of AE=512 keV for electrons and a photon energy cutoff, AP, of 1 keV. Density effect correction factors as those reported in ICRU Report No. 37 (Ref. 64) have been applied. The details of the detectors were provided by the manufacturers. However, for the diode detector the active volume was described as a 50 $\mu$m-thick layer based on the article of Rikner and Grusell,[65] not as a 2.5 $\mu$m-thick layer as indicated in Table I.

In addition to simulation of the detectors, the Monte Carlo code provided theoretical values of $s_{c,p}$ for each collimator calculated as the ratio between the average dose in a small volume of water (a cylinder of 0.1 cm height and 0.025 cm radius) and the correspondent quantity obtained with the reference collimator (60 mm diameter). These theoretical values should represent the "true" $s_{c,p}$ values in the sense that they are independent of the characteristics of the dosimeter used (finite size, materials, perturbation effects).

Based on the level of uncertainty of the Monte Carlo simulations, both the theoretical (true) and simulated values of $s_{c,p}$ have an estimated uncertainty of 0.4% ($2\sigma$). This uncertainty is similar to the precision (reproducibility) of measured $s_{c,p}$ (0.6% at $2\sigma$ for the two microchambers and 0.3% at $2\sigma$ for the two solid state detectors).

By comparing the calculated $s_{c,p}$ for the actual detectors to the theoretical value, it was possible to determine correction factors to be applied to raw data of $s_{c,p}$ as measured by the detectors. The corrected $s_{c,p}$ values should equal their correspondent theoretical values.

The correction factor was defined as[11]

$$F_{\mathrm{corr}}(\phi_{\mathrm{coll}}) = \left( \frac{D_{\phi}^{\mathrm{wat}}/D_{\phi 60\ \mathrm{ref}}^{\mathrm{wat}}}{D_{\phi}^{\mathrm{det}}/D_{\phi 60\ \mathrm{ref}}^{\mathrm{det}}} \right) = \left( \frac{s_{c,p\ \phi}^{\mathrm{wat}}}{s_{c,p\ \phi}^{\mathrm{det}}} \right), \quad (1)$$

where $D_{\Phi}^{\mathrm{det}}$ is the average dose in the active volume of the detector for the collimator used and $D_{\Phi 60\ \mathrm{ref}}^{\mathrm{det}}$ is the dose in the same region for the reference collimator (60 mm diameter). Similar notation is used in the case of simulation in a small volume of water and for $s_{c,p}$.

Previous studies have demonstrated that the most sensitive parameters for beam tuning are the mean energy and the radial intensity distribution of the incident electron beam,[41] that in our case was verified to be properly described by a monochromatic, parallel, Gaussian-distributed beam. The energy was chosen by comparison to experimental TPRs at 10 and 20 cm depth. The value that best matched measured TPRs was 7.0 MeV, in agreement with the specification of the manufacturer. We have also verified that a possible beam energy spread of the electron source, simulated by a Gaussian distribution of the energy with a full width at half maximum (FWHM) of 1 MeV,[73] does not influence beam profiles and gives slightly worse results as to the TPRs.

After initially using beam profiles to fine tune the FWHM of the electron beam distribution, the adopted criterion to estimate the optimal value of the FWHM was the coincidence of measured and simulated $s_{c,p}$ for each detector, as will be explained in the next section.

### II.C. Estimation of $s_{c,p}$

Any Monte Carlo simulation of a radiotherapy treatment unit requires careful determination of source parameters such as energy and radial distribution of the electron beam. In

TABLE II. TPRs measured and calculated for three different energies and for the 5 and 60 mm collimators.

| Depth (cm) | MC calculated TPR coll 5 mm 6.5 MeV | 7 MeV | 7.5 MeV | Measured data | Depth (cm) | MC calculated TPR coll 60 mm 6.5 MeV | 7 MeV | 7.5 MeV | Measured data |
|---|---|---|---|---|---|---|---|---|---|
| 1.5 | 1 | 1 | 1 | 1 | 1.5 | 1 | 1 | 1 | 1 |
| 10 | 0.623 | 0.632 | 0.635 | 0.631 | 10 | 0.725 | 0.732 | 0.747 | 0.732 |
| 20 | 0.363 | 0.379 | 0.381 | 0.379 | 20 | 0.456 | 0.466 | 0.481 | 0.466 |

order to make this study independent from the specific Cyberknife unit under investigation, the following approach was adopted.

Phase spaces with the FWHM of the electron beam distribution of 1.4, 1.8, 2.2, and 2.6 mm have been created for the 5, 7.5, 10, and 60 mm collimators. The specification provided by the manufacturer was the FWHM in the range 1.5–2.0 mm. The simulation was repeated for three different values of electron beam energy: 6.5, 7.0, and 7.5 MeV.

A series of four pairs $(s_{c,p}, F_{\text{corr}})$ was calculated corresponding to the four values of the FWHM, for each energy and collimator; $F_{\text{corr}}$ was calculated for each detector, while $s_{c,p}$ is the true value calculated in water. It was observed that the pairs tend to lay on a straight line (see Fig. 4), with linear correlation coefficients $r$ ranging from 0.984 to 0.999. This pattern establishes a relationship between the true $s_{c,p}$ and $F_{\text{corr}}$; another, independent relationship between these quantities is given by Eq. (1), that can be rewritten as $s_{c,p} = F_{\text{corr}} \cdot s^m_{c,p}$, where $s^m_{c,p}$ is the measured total scatter factor, related to beam parameters of the system under investigation. Finding the intersection between the line defined by the pairs $(s_{c,p}, F_{\text{corr}})$ and the line identified by $s_{c,p} = F_{\text{corr}} \cdot s^m_{c,p}$ (where the measured $s^m_{c,p}$ is interpreted as the slope) provides a means to estimate $F_{\text{corr}}$ and $s_{c,p}$ (represented graphically with an asterisk, $F^*_{\text{corr}}$, $s^*_{c,p}$, in Fig. 4) and, indirectly, to estimate the FWHM of the radial beam distribution for the system on which the measurement has been performed (see Fig. 5). This graphical representation is equivalent to solving the linear system,

$$\begin{cases} F_{\text{corr}} = a\, s_{c,p} + b, \\ s_{c,p} = F_{\text{corr}} s^m_{c,p}, \end{cases} \tag{2}$$

for the variables $F_{\text{corr}}$ and $s_{c,p}$, where $a$ and $b$ result from the linear fit between the pairs $(s_{c,p}, F_{\text{corr}})$ described above.

The results for the Cyberknife unit employed in this study are given in the next section, together with more general data that should allow users to estimate their own parameters based on measurements of TPR and $s^m_{c,p}$. In particular, TPRs should be measured first to estimate beam energy (Table II), then four pairs (FWHM, $s_{c,p}$) should be obtained from Table VI for a given collimator, possibly interpolating between energies. Using Table VII, that associates the FWHM to $F_{\text{corr}}$ for the different detectors, it is possible to determine the four pairs $(s_{c,p}, F_{\text{corr}})$ described above, to be used for the linear fit that would give $a$ and $b$ in Eq. (2). At this point, it is possible to solve Eq. (2) for $s_{c,p}$ (and $F_{\text{corr}}$) using the measured value $s^m_{c,p}$ for the specific Cyberknife unit and, if desired, to obtain the FWHM from Table VI. It must be observed, however, that the small variability in manufacturing (ranging from ±0.02 to ±0.05 mm as communicated by the manufacturers) makes the results of this study usable for the microchambers and the diode detector, while the diamond response depends on the specific shape and dimension of the crystal,[58] thus invalidating the proposed method. For this reason, $F_{\text{corr}}$ values for the diamond detector reported on Table VII shall be considered valid only for the specific detector employed in this study. The actions required to use the data reported here for a Cyberknife system different from the unit investigated in this study are shown in Fig. 2. Note that no further Monte

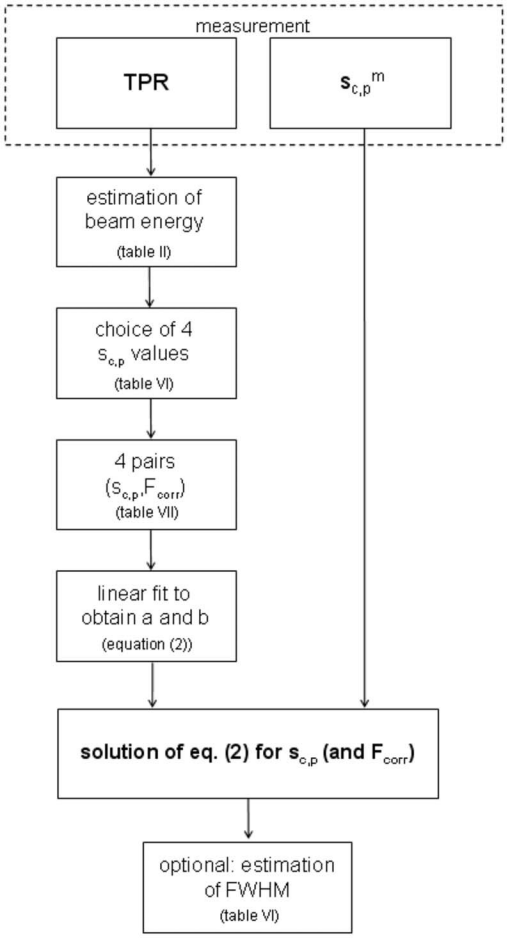


FIG. 2. Flowchart of the actions required to use the data reported in this article to determine $s_{c,p}$ of a Cyberknife system different from the unit investigated in this study. Note that no further Monte Carlo simulation is required. The detector shall be of the same type as one of the microchambers or the diode employed in this study.

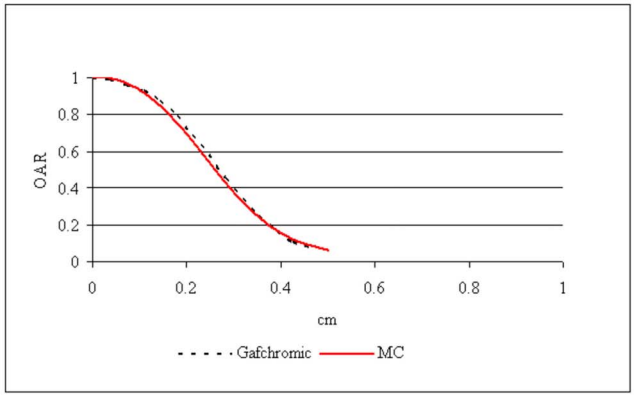


(a)

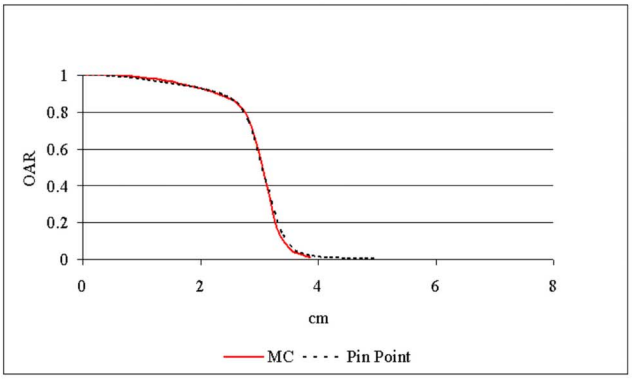


(b)

FIG. 3. (a) and (b) Half-profiles at 1.5 cm depth and SDD=80 cm of the 5 mm diameter collimator (a) and 60 mm diam collimator (b). A comparison between measured profiles (dotted line) and calculated by MC (continuous line) is shown.

Carlo simulation is required.

## III. RESULTS

In Figs. 3(a) and 3(b), normalized half-profiles at 1.5 cm depth and source to detector distance (SDD)=80 cm for the 5 and 60 mm collimators are shown. The profiles obtained with Monte Carlo for the FWHM=2.1 mm and $E$ =7.0 MeV (which were found to be the optimal parameters with the procedure described above) are compared to the measured profiles. The values of the calculated profile have an uncertainty of 0.3% (one standard deviation), while the measured profile with Gafchromic film has an estimated uncertainty of ±1%. The agreement between MC and measurements is within the uncertainties.

In Table II, the calculated and measured TPRs for the 5 and 60 mm collimators are reported. The MC TPRs were calculated in a water phantom at 10 and 20 cm relative to 1.5 cm for a Gaussian radial source with the FWHM=2.1 mm and for electron beam energy of 6.5, 7.0, and 7.5 MeV. The agreement between Monte Carlo and experimental data is within 0.2% for 7.0 MeV. It was also verified that TPR data are not affected by variation of the FWHM of the electron beam within the investigated range (1.4–2.6 mm).

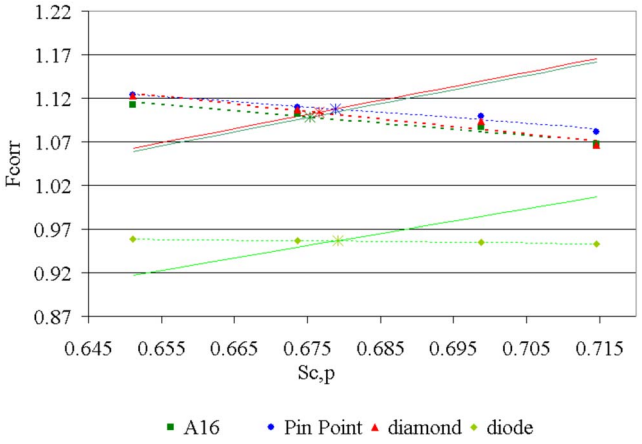


FIG. 4. Correction factors $F_{corr}$ as a function of true Monte Carlo $s_{c,p}$: dotted lines are the linear fit of the calculated $(s_{c,p},F_{corr})$ pairs, continuous lines are the curves whose slope is the inverse of the measured $s_{c,p}$, the symbols identify Monte Carlo calculated pairs $(s_{c,p},F_{corr})$ for the four detectors, and the asterisks represent the intersections between the continuous and the dotted curves for each detector, corresponding to the estimated $s_{c,p}$ and $F_{corr}$.

In Fig. 4, a graphical representation of the method described in the previous paragraph is shown for the 5 mm collimator. The correction factors are represented as a function of the true $s_{c,p}$ calculated with MC for the four different values of the FWHM (smallest $s_{c,p}$ corresponds to the largest FWHM); the different lines refer to the four detectors. The intersection between the continuous line whose slope is the inverse of the measured $s_{c,p}$ $(s_{c,p}^m)$ and the dotted line which is the linear fit between the pairs $(s_{c,p},F_{corr})$ provides the estimated value of $s_{c,p}$ and $F_{corr}$ for the given detector. The four intersections represented by the symbol $*$, give $s_{c,p}$ values ranging from 0.675 to 0.679.

Together with the $s_{c,p}^*$ value for the given collimator, it is possible to estimate the FWHM of the electron beam for the specific Cyberknife unit, by fitting the pairs (FWHM, $s_{c,p}$) and finding the corresponding value of the FWHM, as shown in Fig. 5. For our system, the optimal value of the FWHM

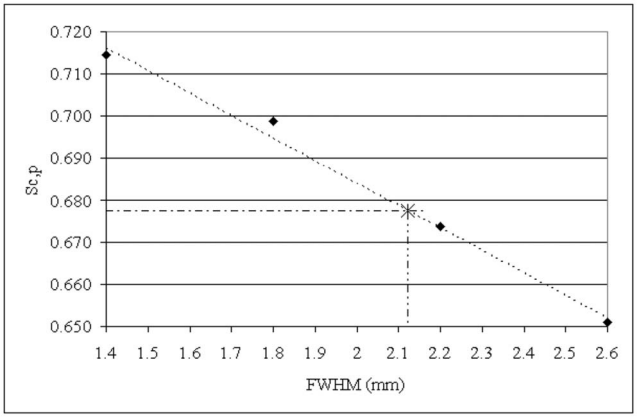


FIG. 5. True Monte Carlo $s_{c,p}$ as a function of the FWHM: the estimated $s_{c,p}^*$ allows the FWHM of the electron beam to be estimated for the Cyberknife system under investigation.

TABLE III. Estimated values of $F^*_{corr}$ and $s^*_{c,p}$ for the 5, 7.5,, and 10 mm collimators, for the four detectors.

| | 5 mm | | 7.5 mm | | 10 mm | |
|---|---|---|---|---|---|---|
| | $F^*_{corr}$ | $s^*_{c,p}$ | $F^*_{corr}$ | $s^*_{c,p}$ | $F^*_{corr}$ | $s^*_{c,p}$ |
| A16 | 1.098 | 0.675 | 1.021 | 0.818 | 1.010 | 0.867 |
| PinPoint | 1.107 | 0.679 | 1.027 | 0.819 | 1.014 | 0.870 |
| Diode | 0.957 | 0.679 | 0.966 | 0.823 | 0.978 | 0.875 |
| Diamond | 1.104 | 0.677 | 1.006 | 0.820 | 1.000 | 0.871 |
| Mean $s_{c,p}$ | | 0.677 | | 0.820 | | 0.871 |
| $\pm 2\sigma$ | | ±0.004 | | ±0.008 | | ±0.008 |

was found to be 2.1 mm. This value has been obtained for the smallest (5 mm) collimator, because its $s_{c,p}$ is the most sensitive to variation of the FWHM. Nevertheless, in order to verify if the method provides consistent results we have calculated the values of the estimated FWHM also for the 7.5 and 10 mm cones. We found the FWHM=2.0 mm and 2.1 mm for the 7.5 and 10 mm cones, respectively.

Table III reports the estimated values of $F^*_{corr}$ and $s^*_{c,p}$ obtained for the four detectors and the three collimators, 5, 7.5, and 10 mm, with the method previously described. The mean $s^*_{c,p}$ and the variation ($2\sigma$) for each collimator are also shown.

In Table IV, the simulated $s_{c,p}$ (that is, $s_{c,p}$ calculated by means of MC by simulating shape and chemical composition of the detectors) has been compared with experimental data for all the detectors. From these results it can be noticed that the measured and the simulated $s_{c,p}$ are coincident only for a particular value of the FWHM of the radial Gaussian distribution of the electron source.

Table V shows raw measurements of $s_{c,p}$ with the four detectors together with the corresponding estimated value, calculated by means of the procedure described in Sec. II using the FWHM=2.1 mm.

In Table VI the Monte Carlo calculated $s_{c,p}$ values (true values) have been reported for the different FWHM and energy parameters, while Table VII reports $F_{corr}$ of the four detectors as a function of the FWHM. Tables II, VI, and VII should be used together as explained at the end of Sec. II C to estimate $s_{c,p}$ for a Cyberknife system different from the specific unit investigated in this study.

## IV. DISCUSSION

Total scatter factors measured with different detectors have shown a variability for the smallest collimators of the Cyberknife system.[5–9] Measured values reported in this study are in agreement with values reported on the literature within the experimental uncertainties. In particular, for the diode

TABLE IV. Measured and MC-simulated $s_{c,p}$, for the four detectors and for the 5, 7.5, and 10 mm collimators, for the various FWHM of the Gaussian spatial distribution of the electron source.

| | | FWHM 1.4 mm | FWHM 1.8 mm | FWHM 2.2 mm | FWHM 2.6 mm |
|---|---|---|---|---|---|
| Coll 5 mm | Measured $s_{c,p}$ | Simulated $s_{c,p}$ | Simulated $s_{c,p}$ | Simulated $s_{c,p}$ | Simulated $s_{c,p}$ |
| A16 | 0.614 | 0.669 | 0.643 | 0.611 | 0.585 |
| PinPoint | 0.613 | 0.661 | 0.636 | 0.607 | 0.582 |
| Diode | 0.710 | 0.757 | 0.732 | 0.704 | 0.679 |
| Diamond | 0.613 | 0.677 | 0.639 | 0.609 | 0.580 |
| Coll 7.5 mm | | | | | |
| A16 | 0.801 | 0.809 | 0.808 | 0.799 | 0.792 |
| PinPoint | 0.798 | 0.805 | 0.802 | 0.795 | 0.789 |
| Diode | 0.852 | 0.757 | 0.850 | 0.843 | 0.842 |
| Diamond | 0.815 | 0.833 | 0.818 | 0.813 | 0.803 |
| Coll 10 mm | | | | | |
| A16 | 0.859 | 0.874 | 0.870 | 0.860 | 0.857 |
| PinPoint | 0.858 | 0.867 | 0.865 | 0.860 | 0.857 |
| Diode | 0.895 | 0.909 | 0.896 | 0.890 | 0.886 |
| Diamond | 0.871 | 0.889 | 0.876 | 0.872 | 0.866 |

TABLE V. Raw measurements and estimated values of $s_{c,p}$ for the 5, 7.5, and 10 mm collimators.

| | 5 mm | | 7.5 mm | | 10 mm | |
|---|---|---|---|---|---|---|
| | Raw $s_{c,p}$ | $s^*_{c,p}$ | Raw $s_{c,p}$ | $s^*_{c,p}$ | Raw $s_{c,p}$ | $s^*_{c,p}$ |
| A16 | 0.615 | 0.675 | 0.801 | 0.818 | 0.859 | 0.867 |
| PinPoint | 0.613 | 0.679 | 0.798 | 0.819 | 0.858 | 0.870 |
| Diode | 0.710 | 0.679 | 0.852 | 0.823 | 0.895 | 0.875 |
| Diamond | 0.613 | 0.677 | 0.815 | 0.820 | 0.871 | 0.871 |
| Mean $s_{c,p}$ | 0.638 | 0.677 | 0.817 | 0.820 | 0.871 | 0.871 |
| $\pm 2\sigma$ | 0.096 | 0.004 | 0.050 | 0.004 | 0.034 | 0.007 |

detector and for the 5 mm collimator, Yu *et al.*[6] found $s_{c,p}=0.719\pm0.015$, compared to 0.710 of the present study; for the 7.5 mm collimator they reported $s_{c,p}=0.849\pm0.012$ and for the 10 mm collimator $s_{c,p}=0.892\pm0.011$, compared to 0.852 and 0.895 of the present study, respectively. Araki *et al.*[5] reported a graphical representation of average $s_{c,p}$ values from 14 Cyberknife units installed in Japan, giving $s_{c,p}=0.72$ for a diode detector and the 5 mm collimator, 0.845 for the 7.5 mm, and 0.885 for the 10 mm collimator. The diode detector employed in those studies was not of the same type reported in this work, however, its characteristics could be considered similar; both detectors were an unshielded-type diode. Wilcox *et al.*[7] reported $s_{c,p}=0.596$ for the A16 microchamber and the 5 mm collimator, compared to 0.615 of the present study. For the 7.5 and 10 mm collimators the values were 0.790 and 0.859, compared to 0.801 and 0.859 of the present study. The discrepancy for the 5 mm collimator might be interpreted as due to difficulties in the experimental setup but also to actual differences in beam parameters or even in the geometry (diameter) of the secondary collimator. Other published studies on total scatter factors of the Cyberknife radiosurgery system are not directly comparable to these results because of the different detectors employed.[8,9] In particular, the data reported by Wilcox *et al.* for the PTW 60008 diode are systematically higher than our results with the PTW 60012 diode, but this is consistent with studies demonstrating an over-response of the shielded-type diode (60008) for scatter factors of small beams.[66]

Possible explanations of variations between reported $s_{c,p}$ values include the type of detector, difficulties in the experimental setup, and actual differences in beam parameters, especially the electron beam width. According to the simulation reported in this study, a difference of 0.5 mm in the electron beam width causes a 4% variation in the scatter factor of the smallest collimator. As regards different detectors, microchambers usually give an underestimation of the scatter factor, while diodes give an overestimation. Also the diamond detector can give an underestimation due to its large volume compared to the collimator size. This variability among detectors can be reduced if correction factors, calculated with the Monte Carlo method indicated in this work, are applied to raw measurements.

Total scatter factors and correction factors ($F_{\mathrm{corr}}$) vary with the dimension of the electron beam (described by the FWHM in this study, see Tables VI and VII), so it is essential to estimate the FWHM correctly before using Monte Carlo to simulate the experimental setup. In order to do that, experimental measurements shall be taken into account. The usual approach of determining the spatial distribution of the electron beam from beam profiles is prone to uncertainties that could potentially invalidate the method. In fact, microchambers are generally affected by problems related to the finite dimension of the active volume that make them unsuitable for measurement in regions of strong gradient. The diode must be used carefully because it can perturb the profiles depending on the direction of its axis with respect to the direction of scanning and on the presence of a metal shield for scattered photons.[66,67] On the other hand, radiographic films are affected by nonuniform spectral sensitivity,[68] and radiochromic films show a statistical uncertainty that is too high to allow small variations of the FWHM to be detected.[7] The profile-matching method is not able to account for small variations of the FWHM because of two types of uncertainty: the detector's characteristics that can influence the measurement of the profile[69–72] and the statistical uncertainty of the Monte Carlo simulation. For the latter, there is no obvious limit on the uncertainty to be reached. In the literature a statistical uncertainty of 1%–2% is often accepted,[1,5,9,14] due to the large amount of computing time for a small voxel size,

TABLE VI. Monte Carlo calculated $s_{c,p}$ for 6.5, 7.0, and 7.5 MeV and for the four values of the FWHM.

| | $E$=6.5 MeV | | | $E$=7.0 MeV | | | $E$=7.5 MeV | | |
|---|---|---|---|---|---|---|---|---|---|
| FWHM | 5 mm | 7.5 mm | 10 mm | 5 mm | 7.5 mm | 10 mm | 5 mm | 7.5 mm | 10 mm |
| 1.4 | 0.726 | 0.834 | 0.890 | 0.715 | 0.826 | 0.882 | 0.709 | 0.822 | 0.878 |
| 1.8 | 0.709 | 0.832 | 0.881 | 0.699 | 0.821 | 0.876 | 0.692 | 0.817 | 0.875 |
| 2.2 | 0.684 | 0.827 | 0.882 | 0.674 | 0.815 | 0.871 | 0.660 | 0.812 | 0.873 |
| 2.6 | 0.663 | 0.820 | 0.880 | 0.651 | 0.813 | 0.866 | 0.635 | 0.805 | 0.870 |

TABLE VII. $F_{corr}$ of the four detectors for the 5, 7.5, and 10 mm collimators, as a function of the FWHM.

| A16 | $F_{corr}$ | | |
|---|---|---|---|
| FWHM (mm) | 5 mm coll | 7.5 mm coll | 10 mm coll |
| 1.4 | 1.067 | 1.021 | 1.008 |
| 1.8 | 1.087 | 1.017 | 1.007 |
| 2.2 | 1.102 | 1.020 | 1.012 |
| 2.6 | 1.112 | 1.027 | 1.010 |
| Pin Point | | $F_{corr}$ | |
| FWHM (mm) | 5 mm coll | 7.5 mm coll | 10 mm coll |
| 1.4 | 1.082 | 1.025 | 1.017 |
| 1.8 | 1.099 | 1.024 | 1.013 |
| 2.2 | 1.110 | 1.025 | 1.013 |
| 2.6 | 1.124 | 1.037 | 1.016 |
| Diode | | $F_{corr}$ | |
| FWHM (mm) | 5 mm coll | 7.5 mm coll | 10 mm coll |
| 1.4 | 0.953 | 0.966 | 0.978 |
| 1.8 | 0.955 | 0.966 | 0.978 |
| 2.2 | 0.957 | 0.967 | 0.978 |
| 2.6 | 0.940 | 0.967 | 0.978 |
| Diamond | | $F_{corr}$ | |
| FWHM (mm) | 5 mm coll | 7.5 mm coll | 10 mm coll |
| 1.4 | 1.066 | 1.001 | 1.001 |
| 1.8 | 1.093 | 1.007 | 1.000 |
| 2.2 | 1.107 | 1.010 | 0.999 |
| 2.6 | 1.123 | 1.012 | 1.001 |

as required in the simulation of small beams. From data obtained in this study, it results that using ±1% uncertainty on calculated profiles would result in an uncertainty on the FWHM of ±0.4 mm, with a consequent uncertainty of ±3% in the total scatter factor of the 5 mm collimator (Fig. 5). In this work, all the simulations have been made with a final uncertainty of ±0.2%−0.3% (one standard deviation) for all voxel sizes.

In a previous work we did not adopt the strategy based on a consistency check between measured and simulated $s_{c,p}$ to fine-tune beam parameters, but we choose the common praxis of benchmarking the simulation against measurement of depth-dose curves and beam profiles.[4] We believe that the new approach is more sensitive to small variations of beam width, which are likely to occur and which have a demonstrated, significant influence on scatter factors (see, e.g., Fig. 5, where a variation of 4% occurs in the scatter factor as a consequence of a 0.5 mm variation in beam width). Furthermore, the method proposed in this work is not sensitive to the specific detector used for profile measurement, as confirmed by the consistent values of the FWHM obtained with the different detectors. We preferred to combine simulation and experimental measurements by means of the method described above. This approach should overcome criticisms that are often correctly addressed to pure Monte Carlo methods in the determination of total scatter factors of small beams.[38] With the proposed method, the whole source-detector system is subject to simulation, and experimental measurements of $s_{c,p}$ are used to check simulations for consistency. In fact, once the energy has been chosen by means of TPR comparison, there is only one value (or a narrow interval of values) of the FWHM that makes simulation consistent with experimental results, provided that not only the "ideal detector" made of a small volume of water but also the actual detectors are simulated. It was also shown that results in terms of corrected $s_{c,p}$ are consistent to each other if different detectors are considered, either affected by under-response (microchambers and diamond) or over-response (diode).

The estimated correction factors are greater than 1 for the microchambers and the diamond detector, while $F_{corr}$ for the diode detector is smaller than 1. This is interpreted as a prevalence of volume effects for the microchambers and the diamond and as an effect due to the high atomic number of the active layer and the surrounding silicon substrate for the diode.

From the results of this study there is no clear indication on which should be the detector of choice. It must be emphasized that no ideal detector exists. Usually, the characteristics of the different detectors are analyzed and compared from the experimental point of view, in particular evaluating their performances for the specific type of measurement (profiles, total scatter factor, or depth dose curves). The characteristics that render a detector suitable for the method presented here differ in general from those required for its use without Monte Carlo correction. In fact, the main factors that must be considered in this case are the reproducibility in manufacturing of the detector in order to have the correction factor applicable for all the detectors of the same type, and the dependence of the correction factor on the FWHM of the electron beam source, chosen for the MC simulation of the treatment head. The energy dependence of the diode is a concern if the detector is used without any correction factor, but is supposed to be adequately accounted for by MC simulation. The diode was also the less sensitive to the FWHM variations, however, it suffers from a poorer definition of the actual dimensions of the active volume in both depth and front area, which renders the simulation more uncertain compared to microchambers. The diamond is affected by significant variability in shape, which makes the results of this study valid only for the specific detector used. On the other hand, microchambers offer an adequate manufacturing accuracy to allow a single simulation to be used for all the detectors of the same type, however, their correction factors show greater dependence on the spatial distribution of the electron beam. The method described in Sec. II C might offer a means to overcome this difficulty.

## V. CONCLUSIONS

In conclusion, the scope of this study was to estimate total scatter factors of the three smallest collimators of the Cyberknife radiosurgery system (5–10 mm in diameter), com-

bining experimental measurements and Monte Carlo simulation. It was found that total scatter factors vary with the spatial distribution of the electron beam incident on the target, and a method was adopted to estimate the correct values of $s_{c,p}$, together with the FWHM of the electron beam and correction factors to be applied to the four detectors employed in the measurement of $s_{c,p}$. Estimations of the FWHM with different collimators and different detectors seem to be in excellent agreement. Measured profiles are also consistent with the estimated value of the FWHM, even if small variations in the FWHM would hardly be detected by considering only their effect on profiles.

The results of this study may be used to estimate $s_{c,p}$ of a Cyberknife system different from the unit investigated in this study. This requires that one of the detectors employed in this study is used, apart from the diamond detector because of excessive manufacturing variability.

To date, the method has been applied only to the Cyberknife radiosurgery system. Further investigation is needed to test whether the method would be applicable to other situations where small beams play an important role, in radiosurgery as well as in intensity modulated radiation therapy.

[a]Electronic mail: pfrancescon@fisica-vicenza.it

[1]G. X. Ding, D. M. Duggan, and C. W. Coffey, "Commissioning stereotactic radiosurgery beams using both experimental and theoretical methods," Phys. Med. Biol. **51**, 2549–2566 (2006).
[2]International Commission on Radiation Units and Measurements, Report No. 62: Prescribing, Recording and Reporting Photon Beam Therapy, 1999.
[3]P. Francescon, C. Cavedon, P. Scalchi, S. Cora, N. Satariano, P. Polloniato, and E. Berna, "TU-C-224C–07: A comprehensive dosimetric protocol for the Cyberknife Radiosurgery System," Med. Phys. **33**, 2194 (2006).
[4]P. Francescon, S. Cora, C. Cavedon, P. Scalchi, and J. Stancanello, in *Robotic Radiosurgery*, edited by R. F. Mould (The Cyberknife Society Press, Sunnyvale, California, 2005), Vol. I, pp. 71–80.
[5]F. Araki, "Monte Carlo study of a Cyberknife stereotactic radiosurgery system," Med. Phys. **33**, 2955–2963 (2006).
[6]C. Yu, J. Gabor, M. Apuzzo, and P. Zbigniew, "Measurements of the relative output factors for CyberKnife collimators," Neurosurgery **54**, 157–162 (2004).
[7]E. E. Wilcox and G. M. Daskalov, "Evaluation of GAFCHROMIC® EBT for Cyberknife® dosimetry," Med. Phys. **34**, 1967–1974 (2007).
[8]J. Deng, C.-M. Ma, J. Hai, and R. Nath, "Commissioning 6 MV photon beams of a stereotactic radiosurgery system for Monte Carlo treatment planning," Med. Phys. **30**, 3124–3134 (2003).
[9]J. Deng, T. Guerrero, C.-M. Ma, and R. Nath, "Modelling 6 MV photon beams of a stereotactic radiosurgery system for Monte Carlo treatment planning," Phys. Med. Biol. **49**, 1689–1704 (2004).
[10]C. Yeboah, "Measurement of linear accelerator photon beam spot size and assessment of its long-term stability," Med. Phys. **33**, 2041 (2006).
[11]P. Francescon, S. Cora, C. Cavedon, P. Scalchi, and S. Reccanello, "Use of a new type of radiochromic film, a new parallel-plate micro-chamber, MOSFETs, and TLD 800 microcubes in the dosimetry of small beams," Med. Phys. **25**, 503–511 (1998).
[12]W. U. Laub and T. Wong, "The volume effect of detectors in the dosimetry of small fields used in IMRT," Med. Phys. **30**, 341–347 (2003).
[13]M. Westermark, J. Arndt, B. Nilsson, and A. Brahme, "Comparative dosimetry in narrow high-energy photon beams," Phys. Med. Biol. **45**, 685–702 (2000).
[14]F. Haryanto, M. Fippel, W. Laub, O. Dohm, and F. Nüsslin, "Investigation of photon beam output factors for conformal radiation therapy-Monte Carlo simulations and measurements," Phys. Med. Biol. **47**, N133–N143 (2002).
[15]L. B. Leybovich, A. Sethi, and N. Dogan, "Comparison of ionization chambers of various volumes for IMRT absolute dose verification," Med. Phys. **30**, 119–123 (2003).
[16]R. K. Rice, J. L. Hansen, G. K. Svensson, and R. L. Siddon, "Measurements of dose distribution in small beams of 6 MV x-rays," Phys. Med. Biol. **32**, 1087–1099 (1987).
[17]C. H. Sibata, H. C. Mota, A. S. Beddar, P. D. Higgins, and K. H. Shin, "Influence of detector size in photon beam profile measurements," Phys. Med. Biol. **36**, 621–631 (1991).
[18]M. Heydarian, P. W. Hoban, and A. H. Beddoe, "A comparison of dosimetry techniques in stereotactic radiosurgery," Phys. Med. Biol. **41**, 93–110 (1996).
[19]M. Stasi, B. Baiotto, G. Barboni, and G. Scielzo, "The behavior of several microionization chambers in small intensity modulated radiotherapy fields," Med. Phys. **31**, 2792–2795 (2004).
[20]C. Martens, C. De Vagter, and W. De Neve, "The value of the Pin Point ion chamber for characterization of small fields segments use in intensity-modulated radiotherapy," Phys. Med. Biol. **45**, 2519–2530 (2000).
[21]D. M. Duggan and C. W. Coffey, "Small photon field dosimetry for stereotactic radiosurgery," Med. Dosim. **23**, 153–159 (1998).
[22]H. D. Kubo, R. B. Wilder, and C. T. Pappas, "Impact of collimator leaf width on stereotactic radiosurgery and 3D conformal radiotherapy plans," Int. J. Radiat. Oncol. Biol. Phys. **44**, 937–945 (1999).
[23]J. S. Tsai, M. J. Rivard, M. J. Engler, J. E. Mignano, D. E. Wazer, and W. A. Shucart, "Determination of the 4 mm gamma knife helmet relative output factor using a variety of detectors," Med. Phys. **30**, 986–992 (2003).
[24]X. R. Zhu, J. J. Allen, J. Shi, and W. E. Simon, "Total scatter factors and tissue maximum ratios for small radiosurgery fields: Comparison of diode detectors, a parallel-plane ion chamber, and radiographic film," Med. Phys. **27**, 472–477 (2000).
[25]E. Pappas, T. G. Maris, A. Papadakis, F. Zacharopoulou, J. Damilakis, N. Papanikolau, and N. Gourtsoyiannis, "Experimental determination of the effect of detector size on profile measurements in narrow photon beams," Med. Phys. **33**, 3700–3710 (2006).
[26]H.-R. Lee, M. Pankuch, and J. C. Chu, "Evaluation and characterization of parallel-plate microchamber's functionalities in small beam dosimetry," Med. Phys. **29**, 2489–2496 (2002).
[27]C. McKerracher and D. I. Thwaites, "Assessment of a new small-field detectors against standard-field detectors for practical stereotactic beam data acquisition," Phys. Med. Biol. **44**, 2143–2160 (1999).
[28]L. B. Leybovich, A. Sethi, and N. Dogan, "Comparison of ionization chambers of various volumes for IMRT absolute dose verifcation," Med. Phys. **30**, 119–123 (2003).
[29]G. X. Ding, "Using Monte Carlo simulations to commission photon beam output factors—A feasibility study," Phys. Med. Biol. **48**, 3865–3874 (2003).
[30]G. X. Ding, "An investigation of accelerator head scatter and output factor in air," Med. Phys. **31**, 2527–2533 (2004).
[31]R. Capote, F. Sanchez-Doblado, A. Leal, J. I. Lagares, R. Arrans, and G. H. Hartmann, "An EGSnrc Monte Carlo study of the microionization chamber for reference dosimetry of narrow irregular IMRT beamlets," Med. Phys. **31**, 2416–2422 (2004).
[32]F. Verhaegen, I. J. Das, and H. Palmans, "Monte Carlo dosimetry study of a 6 MV stereotactic radiosurgery unit," Phys. Med. Biol. **43**, 2755–2768 (1998).
[33]A. Chaves, M. C. Lopes, C. C. Alves, C. Oliveira, L. Peralta, P. Rodrigues, and A. Trinidade, "Basic dosimetry of radiosurgery narrow beams using Monte Carlo simulations: A detailed study of depth of maximum dose," Med. Phys. **30**, 2904–2911 (2003).
[34]K. De Vlamynck, H. Palmans, F. Verhaegen, C. De Vagter, W. De Neve, and H. Thierens, "Dose measurements compared with Monte Carlo simulations of narrow 6 MV multileaf collimator shaped photon beams," Med. Phys. **26**, 1874–1882 (1999).
[35]T. Yamamoto, T. Teshima, S. Miyajima, M. Matsumoto, H. Shiomi, T. Inoue, and I. Hirayama, "Monte Carlo calculation of depth doses for small field of Cyberknife," Radiat. Med. **20**, 305–310 (2002).
[36]D. W. O. Rogers, B. A. Faddegon, G. X. Ding, C.-M. Ma, J. We, and T. R. Mackie, "BEAM: a Monte Carlo code to simulate radiotherapy treatment units," Med. Phys. **22**, 503–524 (1995).
[37]D. Sheikh-Bagheri, D. W. O. Rogers, C. K. Ross, and J. P. Seuntjens, "Comparison of measured and Monte Carlo calculated dose distributions from the NRC linac," Med. Phys. **27**, 2256–2266 (2000).
[38]O. A. Sauer and J. Wilbert, "Measurement of output factors for small photon beams," Med. Phys. **34**, 1983–1988 (2007).

[39]J. R. Adler, Jr., S. D. Chang, M. J. Murphy, J. Doty, P. Geis, and S. L. Hancock, "The Cyberknife: A frameless robotic system for radiosurgery," Stereotact. Funct. Neurosurg. **69**, 124–128 (1997).
[40]H. Bouchard and J. P. Seuntjens, "Ionization chamber-based reference dosimetry, of intensity modulated radiation beams," Med. Phys. **31**, 2454–2465 (2004).
[41]D. Sheikh-Bagheri and D. W. O. Rogers, "Sensitivity of megavoltage photon beam Monte Carlo simulations to electron beam and other parameters," Med. Phys. **29**, 379–390 (2002).
[42]M. K. Fix, P. J. Keall, K. Dawson, and J. V. Siebers, "Monte Carlo source model for photon beam radiotherapy: Photon source characteristics," Med. Phys. **31**, 3106–3121 (2004).
[43]G. Rikner and E. Grusell, "General specifications for silicon semiconductors for use in radiation dosimetry," Phys. Med. Biol. **32**, 1109–1117 (1987).
[44]A. S. Saini and T. C. Zhu, "Temperature dependence of commercially available diode detectors," Med. Phys. **29**, 622–630 (2002).
[45]A. S. Saini and T. C. Zhu, "Dose rate and SDD dependence of commercially available diode detectors," Med. Phys. **31**, 914–924 (2004).
[46]*TG-62, Diode in vivo dosimetry for patients receiving external beam radiation therapy Report of the AAPM radiation therapy committee Task Group No. 62* (Medical Physics Publishing, Madison, WI, 2005).
[47]C. McKerracher and D. I. Thwaites, "Assessment of new small-field detectors against standard-field detectors for practical stereotactic beam data acquisition," Phys. Med. Biol. **44**, 2143–2160 (1999).
[48]C. McKerracher and D. I. Thwaites, "Notes on the construction of solid-state detectors," Radiother. Oncol. **79**, 348–351 (2006).
[49]P. Björk, T. Knöös, and P. Nilsson, "Comparative dosimetry of diode and diamond detectors in electron beams for intraoperative radiation therapy," Med. Phys. **27**, 2580–2588 (2000).
[50]S. Vatnitsky and H. Järvinen, "Application of natural diamond detector for the measurement of relative dose distributions in radiotherapy," Phys. Med. Biol. **38**, 173–184 (1993).
[51]M. Heydarian, P. W. Hoban, W. A. Beckham, I. A. Borchardt, and A. H. Beddoe, "Evaluation of a PTW diamond detector for electron beam measurements," Phys. Med. Biol. **38**, 1035–1042 (1993).
[52]P. W. Hoban, M. Heydarian, W. A. Beckham, and A. H. Beddoe, "Dose rate dependence of a PTW diamond detector in the dosimetry of a 6 MV Photon beam," Phys. Med. Biol. **39**, 1219–1229 (1994).
[53]V. S. Khrunov, S. S. Martynov, S. M. Vatnisky, I. A. Ermakov, A. M. Chervjakov, D. L. Karlin, V. I. Fominych, and Y. V. Tarbeyev, "Diamond detectors in relative dosimetry of photon, electron and proton radiation fields," Radiat. Prot. Dosimetry **33**, 155–157 (1990).
[54]W. U. Laub, T. W. Kaulich, and F. Nusslin, "Energy and dose rate dependence of a diamond detector in the dosimetry of 4-25 MV photon beams," Med. Phys. **24**, 535–536 (1997).
[55]X. R. Zhu, J. J. Allen, J. Shi, and W. E. Simon, "Total scatter factors and tissue maximum ratios for small radiosurgery fields: Comparison of diode detectors, a parallel-plate ion chamber, and radiographic film," Med. Phys. **27**, 472–477 (2000).
[56]M. Bucciolini, F. Banci Buonamici, S. Mazzocchi, C. De Angelis, S. Onori, and G. A. P. Cirrone, "Diamond detector versus silicon diode and ion chamber in photon beams of different energy and field size," Med. Phys. **30**, 2149–2154 (2003).
[57]S. Onori, C. De Angelis, P. Fattibene, M. Pacilio, E. Petetti, L. Azario, R. Miceli, A. Piermattei, L. Barone Tonghi, G. Cuttone, and S. Lo Nigro, "Dosimetric characterization of silicon and diamond detectors in low-energy proton beams," Phys. Med. Biol. **45**, 3045–3058 (2000).
[58]C. De Angelis, S. Onori, M. Pacilio, G. A. Cirrone, G. Cuttone, L. Raffaele, M. Bucciolini, and S. Mazzocchi, "An investigation of the operating characteristics of two PTW diamond detectors in photon and electron beams," Med. Phys. **29**, 248–254 (2002).
[59]I. Kawrakow, D. W. O. Rogers, and B. Walters, "Large efficiency improvements in BEAMnrc using directional bremsstrahlung splitting," Med. Phys. **31**, 2883–2898 (2004).
[60]I. Kawrakow and D. W. O. Rogers, "The EGSnrc Code System: Monte Carlo simulation of electron and photon transport," *Technical Report PIRS-701* (4th printing) (National Research Council of Canada, Ottawa, Canada, 2003).
[61]I. Kawrakow, "Accurate condensed history Monte Carlo simulation of electron transport. I. EGSnrc the new EGS4 version," Med. Phys. **27**, 485–498 (2000).
[62]I. Kawrakow, "EGSnrc C++ class library," *Technical Report PIRS-898* (National Research Council of Canada, Ottawa, Canada, 2005).
[63]I. Kawrakow, "On the effective point of measurement in megavoltage photon beams," Med. Phys. **33**, 1829–1839 (2006).
[64]ICRU, "Stopping powers for electrons and positrons," *ICRU Report No. 37* (ICRU, Washington, DC, 1984).
[65]G. Rikner and E. Grusell, "Effects of radiation damage on *p* -type silicon detectors," Phys. Med. Biol. **28**, 1261–1267 (1983).
[66]I. Griessbach, M. Lapp, J. Bohsung, G. Gademann, and D. Harder, "Dosimetric characteristics of a new unshielded silicon diode and its application in clinical photon and electron beams," Med. Phys. **32**, 3750–3754 (2005).
[67]A. S. Beddar, D. J. Mason, and P. F. O'Brian, "Absorbed dose perturbation caused by diodes for small field photon dosimetry," Med. Phys. **21**, 1075–1079 (1994).
[68]X. R. Zhu, S. Yoo, P. A. Jursinic, D. F. Grimm, F. Lopez, J. J. Rownd, and M. T. Gillin, "Characteristics of sensitometric curves of radiographic films," Med. Phys. **30**, 912–919 (2003).
[69]G. Bednarz, S. Huq, and U. Rosenow, "Deconvolution of detector size effect for output factor measurement for narrow Gamma Knife radiosurgery beams," Phys. Med. Biol. **47**, 3643–3649 (2002).
[70]P. D. Higgins, C. H. Sibata, L. Siskind, and J. W. Sohn, "Deconvolution of detector size effect for small field measurement," Med. Phys. **22**, 1663–66 (1995).
[71]F. Garcia-Vicente, J. M. Delgado, and C. Peraza, "Experimental determination of the convolution kernel for the study of the spatial response of a detector," Med. Phys. **25**, 202–207 (1998).
[72]W. Ulmer and W. Kaissl, "The inverse problem of a Gaussian convolution and its application to the finite size of the measurement chambers/detectors in photon and proton dosimetry," Phys. Med. Biol. **48**, 707–727 (2003).
[73]Accuray, Inc. (private communication).